Malaysian Journal of Chemistry, 2024, Vol. 26(3), 347-361
(Special Issue: *3rd Virtual International Symposium on Sciences 2023*)

Synthesis of HTMS-HTES Hydrophobic Coating for Cotton and Polyester Fabrics via Sol-Gel Method

Nurul Hidayah Abu Bakar and Wan Norfazilah Wan Ismail*
Faculty of Industrial Sciences and Technology, Universiti Malaysia Pahang Al-Sultan Abdullah, Lebuh Persiaran Tun Khalil Yaakob, 26300, Paya Besar, Kuantan, Pahang Darul Makmur, Malaysia
***Corresponding author (e-mail: norfazilah@umpsa.edu.my)**

Hydrophobic coatings, inspired by the lotus effect, are favoured for repelling water and addressing challenges such as self-cleaning, oil/water separation, anti-icing, and stain resistance. Key requirements include nanoscale roughness and low surface energy materials. However, fluorinated chemicals in these coatings raise environmental concerns, prompting a demand for water-based alternatives. Producing water-based hydrophobic coatings poses challenges related to synthesising stable dispersions of low surface energy materials and identifying water-soluble adhesives. This study focuses on developing water-based hydrophobic coatings for cotton and polyester textiles using hexyltrimethoxysilane (HTMS) and hexyltriethoxysilane (HTES) via a sol-gel method. Hydrophobic properties were assessed through water contact angle (WCA) measurements and wettability observations. Fourier transform infrared spectroscopy (FTIR) analysed functional groups while scanning electron microscopy-energy dispersive X-ray analysis (SEM-EDX) examined surface morphology and elemental composition. Results showed favourable hydrophobic properties with HTMS-HTES coatings, as water droplets formed spherical shapes without penetrating fabric surfaces. WCA values reached 135.41° for cotton and 132.28° for polyester fabric at a 1:0.6 HTMS:HTES molar ratio, indicating enhanced hydrophobicity. FTIR confirmed siloxane Si–O–Si bond formation, and SEM-EDX indicated good adhesion, promising water-repellent textiles for various industries.

Keywords: Sol-gel method; water-based coating; self-cleaning surface; hydrophobic cotton; hydrophobic polyester

Received: October 2023; Accepted: February 2024

Hydrophobic coatings function to resist water by integrating the characteristics of the "lotus effect" into material surfaces. The "Lotus effect," characterized by lotus leaves allowing water droplets to roll off effortlessly while keeping the surface clean, has received significant attention among researchers. Due to its capacity to tackle a range of applications including self-cleaning, separating oil and water, preventing ice formation, and resisting stains and dust hydrophobic surfaces, which were inspired by such phenomenon, has gained popularity in recent years [1, 2]. In order to produce a hydrophobic surface, it is essential to fulfill two key requirements which are having nanoscale roughness and utilising materials with low surface energy (LSE) [3, 4]. Adapting nanoparticles such as nano-ZnO, nano-SiO_2, nano-CuO, or nano-graphene oxide can provide nanoscale roughness, meanwhile, the addition of long-chained hydrocarbons or material comprising fluorine to the surface of the substrate can produce the necessary LSE. When these factors work together, the fabric surface ought to exhibit a WCA of more than 90° [5].

Previous research on hydrophobic fabrics has found that fluorine-based coatings are 10 to 40 times more environmentally damaging than alternative compounds such as silica and titanium [6]. Given these environmental issues, there is a thriving industry for water-based hydrophobic coatings. Synthesising water-based hydrophobic coatings poses two major obstacles. Firstly, achieving a stable dispersion of LSE materials in water is not easy. Secondly, while using adhesive enhances the durability and longevity of coatings, most silicone-based adhesives that bond the coating to the underlying substrate can only dissolve in organic solvents [7]. In this study, methods of dissolution of LSE materials and adhesives in water were explored, aiming to develop a solvent-free formulation for a hydrophobic coating using the sol-gel method.

Hexyltrimethoxysilane (HTMS) with hexyltriethoxysilane (HTES) are silanes known for their hydrophobic properties. These silanes feature hydrophobic alkyl chains attached to silicon atoms, enabling them to form hydrophobic coatings on various substrates. The use of HTMS and HTES has been explored for various applications such as self-cleaning surfaces, anti-fouling coatings, and water-repellent fabrics. However, the application of these silanes for the production of hydrophobic coatings remains relatively limited compared to other silica-based precursors such as

†Paper presented at the 3rd Virtual International Symposium on Sciences (3rd VISoS 2023)

tetraethylorthosilicate. Nevertheless, HTMS and HTES both have the potential to create coatings that are structurally stable and highly hydrophobic [8].

Hydrophobic solutions may be produced using several approaches, including sol-gel process, polymerization and surface modification. Sol-gel technique stands out as a convenient and effective approach to formulating hydrophobic coating solutions by using materials like silica, alumina, and titania [9]. In comparison to other approaches, sol-gel offers advantages like the ability to be operated at low temperatures, easy adjustment of coating composition and thickness and the flexibility to customise the surface parameters of the coating. As a result, it is considered to be among the most adaptable and widely applied techniques for synthesizing hydrophobic coatings [10].

Textile coating employs a variety of coating techniques. Major techniques include screen printing, evaporation methods, spray techniques, layer-layer deposition, plasma coating, UV coating, chemical and physical vapour deposition, inkjet coating, knife coating, and dip and pad coating [11]. The dip coating process involves immersion of the substrate fabric into a solution that contains adhesive, nanoscale roughness structures and LSE compounds. The coating reaction is then allowed to develop, facilitating the addition of LSE materials and rough nanoscale textures to a variety of textiles. Also, it is straightforward and does not require expensive breakthrough technology [3, 12].

In this research, water-based hydrophobic coating utilizing HTMS and HTES as precursors were synthesised via a one-step sol-gel method in acidic conditions. The dip-pad-cure technique was used to apply solutions with seven different molar ratios of HTMS:HTES to cotton and polyester textiles. After that, the textiles were cured at room temperature. The effect of precursor molar ratios on the hydrophobic properties of the treated fabric samples were evaluated through observation. WCA measurement with a contact angle detector was used to further assess the static wettability of the coated fabric samples. Functional groups were examined using Fourier transform infrared spectroscopy (FTIR) in both raw materials and the optimised coating solutions. Energy dispersive X-ray analysis and scanning electron microscopy (SEM-EDX) were used to compare the surface morphology and elemental composition of coated and untreated fabric samples.

EXPERIMENTAL

Chemicals and Materials

Plain-woven white cotton fabric with a thickness of 120 gsm, and white polyester fabric woven in twill with a thickness of 180 gsm, were procured from a local fabric store. Hexyltrimethoxysilane (HTMS), $C_9H_{22}O_3Si$ (97%, industrial grade), hexyltriethoxysilane (HTES), $C_{12}H_{28}O_3Si$ (99%, industrial grade), and dibutyl dilaurate (DBTDL), $(CH_3(CH_2)_{10}CO_2)_2Sn((CH_2)_3CH_3)_2$ (95%) were purchased from KHL Global Sdn Bhd. Hydrochloric acid, HCl (fuming 37%) was obtained from R&M Chemicals. Denatured ethanol (95%) used to remove dirt from fabrics was purchased from DChemie Chemicals Supply. De-ionized water served as a solvent and for washing.

Synthesis of Modified SiO_2 Hydrosol

A water-based HTMS solution was prepared using the sol-gel method referring to the method from the previous study [13, 14] by mixing it with 0.1 M hydrochloric acid and deionized water on a hotplate stirrer at 450 rpm and 30 °C. The molar ratio of HTMS to water was fixed at 1:3, while the volume of HCl was fixed at 5% of the volume of HTMS. After a clear solution was obtained for about 20 minutes, DBTDL was added and stirred until a clear solution was obtained. The DBTDL volume was fixed at 125 µL. Finally, HTES was added and stirred until homogeneity was achieved and the solution was ready for coating. Observations for hydrophobicity were executed by adding a few water droplets to the treated fabric samples and left for about an hour to determine the water penetration.

Table 1. Variations of HTMS-HTES formulation.

No	HTMS volume, µL	HTES volume, µL	HTMS:HTES ratio
1	5000	0	1:0.00
2	5000	750	1:0.15
3	5000	1500	1:0.30
4	5000	2250	1:0.45
5	5000	3000	1:0.60
6	5000	3750	1:0.75
7	5000	4500	1:0.90

Treatment of Fabrics

Deploying the treatment method from [14], cotton and polyester fabric samples were cut into squares with dimension of 3 cm × 3 cm [15]. These samples were then pre-treated with ethanol for 10 minutes at 29 °C to clean and remove dirt using a DSA ultrasonic cleaner. The modified SiO_2 hydrosols were coated onto the fabric samples by the dip-pad-cure process. The fabrics were immersed in the SiO_2 coating solution for 10 minutes and then padded using Testex TD110 Lab Wringer (Padder) with a 0.9072 kg weight.

Characterization

The static wetting properties of the coated fabric samples were assessed by measuring the WCA using 5 µL water droplets at room temperature. This analysis was performed using the OCA40 contact angle analyser (Dataphysics, Germany), equipped with a 5 µL syringe and an 18G needle. To analyse the functional group present in liquid samples, the Perkin Elmer Fourier Transform Infrared Spectroscopy (FTIR) Spectrophotometer was employed. Spectra were collected in the range of 4000 to 700 cm^{-1} with a resolution of 4 cm^{-1}. FTIR analysis was carried out on the raw materials (HTMS, HTES), hydrolysed HTMS and the optimized coating solution sample to detect any changes in functional groups due to hydrolysis and other chemical reactions during the sol-gel process. For liquid samples, Attenuated Total Reflection (ATR) was employed to obtain FTIR spectra. Furthermore, the surface morphology and elemental composition of both coated and uncoated fabrics were investigated using a Hitachi TM3030 Plus SEM-EDX at 10 kV, with a resolution ranging from 5 µm to 50 µm.

RESULTS AND DISCUSSION

Mechanism in Coating Solution

In this study, HTMS-HTES hydrophobic coatings were synthesized using the sol-gel method. Additionally, the effects of seven different molar ratios of HTMS: HTES on the hydrophobic performance of the coatings were investigated. The preparation of HTMS-HTES coating commenced with the initiation of the hydrolysis of HTMS using water. During this process, the methoxy groups (OCH_3) of HTMS were replaced by hydroxyl groups (OH) from water, resulting in the formation of silanol groups (Si-OH) (Figure 1). Under acidic conditions, hexylsilanetriol and methanol were generated as by-products of the hydrolysis reaction [16].

DBTDL served as a catalyst for the formation of siloxane bonds (Si–O–Si) in the condensation reaction between HTMS and HTES, thereby acting as the cross- linking agent for the two precursors. The DBTDL, a tin catalyst, mediated the condensation reaction by removing the – OH group in HTMS and HTES through a tin catalyst mechanism [17]. DBTDL was first hydrolysed with water to produce organotin hydroxide. Organotin hydroxide then reacted with hexylsilanetriol to form organotin silanolate (Figure 2). Upon adding HTES into the solution, it underwent hydrolysis by reacting with water and methanol (Figure 3) [18]. Notably, the water and methanol involved in the reaction were not added separately but rather originated as by-products from previous reactions. Subsequently, the organotin silanolate reacted with HTMS and crosslinked with HTES through a Si–O–Si bridge (Figure 4).

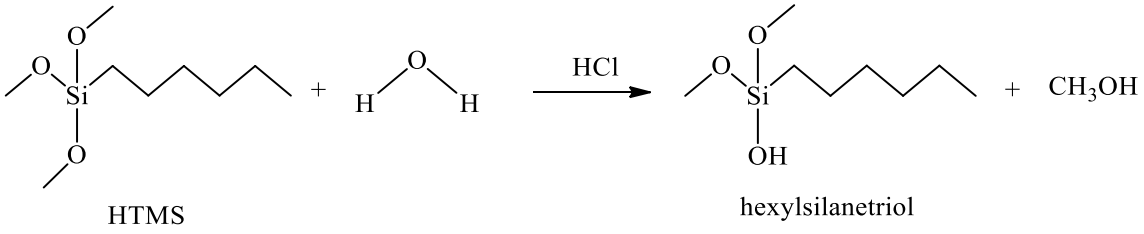

Figure 1. Hydrolysis of HTMS produces hexylsilanetriol and methanol [16].

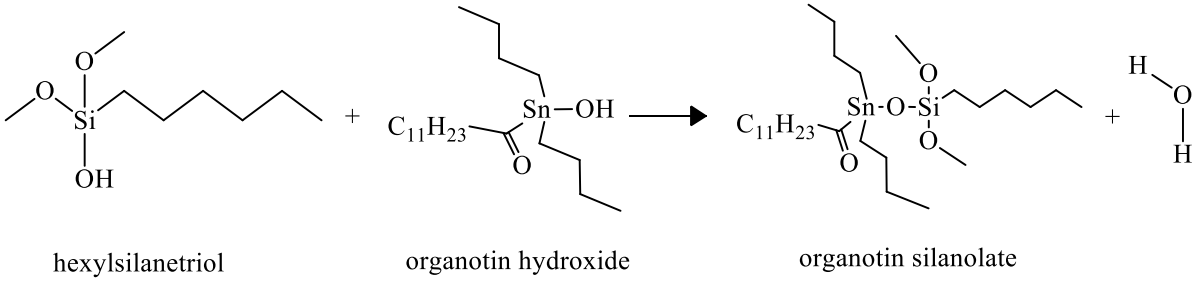

Figure 2. Organotin hydroxide reacts with hexylsilanetriol to form organotin silanolate.

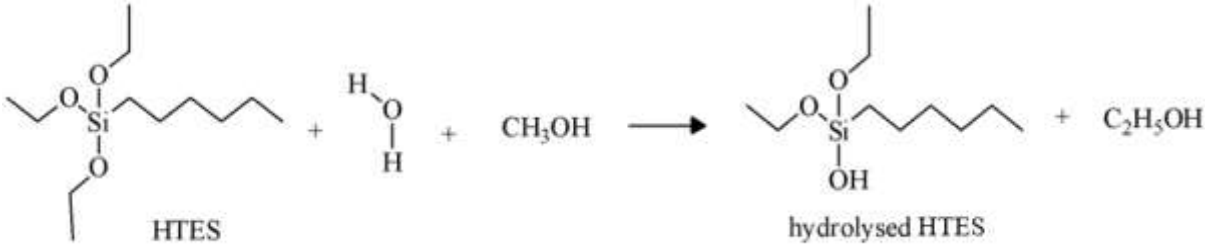

Figure 3. Hydrolysation of HTES with the aid of methanol, a by-product from HTMS hydrolysation [18].

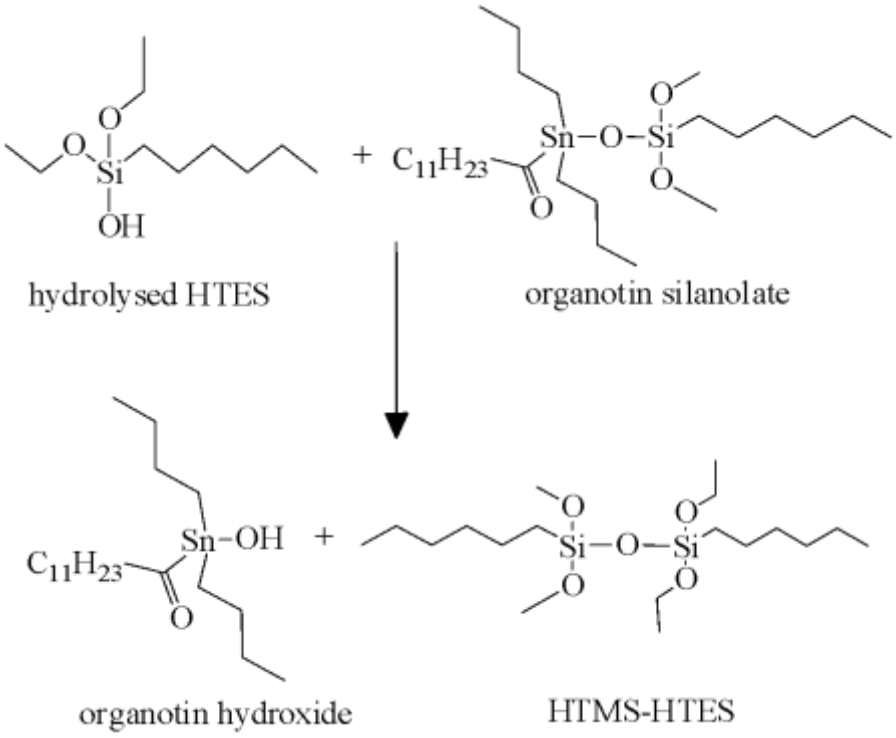

Figure 4. The reaction of organotin silanolate with hydrolysed HTES to form a Si–O–Si bond.

The polycondensation reaction of HTMS and HTES, creating a silicone network, is shown in Figure 5. Once formed, this network polymer adheres to the fabric surface and forms a covering layer through hydrogen bonding for cotton and dipole-dipole bonding for polyester.

Referring to Figure 6, hydrogen bonds are formed by attractive interactions between a hydrogen atom and another atom in the -X-H form, where X is an electronegative atom such as nitrogen, oxygen, or a fluorine atom [19].

In the case of polyester, dipole-dipole bonding takes place between the oxygen atom in the C=O group of the polyester molecules and the hydrogen atom in the C-H group of the coating molecules [20], as illustrated in Figure 7.

Wettability of Coated Fabric Surface

The WCA principle measures the angle between a liquid drop and a solid surface, indicating surface wettability. It reflects molecular interactions, with smaller angles suggesting better wetting. A surface is considered hydrophobic when the WCA value is more than 90°. The hydrophobicity of the coated fabrics was observed by adding a few water droplets and leaving them for about an hour to determine water penetration. These surfaces were determined by their respective HTMS to HTES molar ratios.

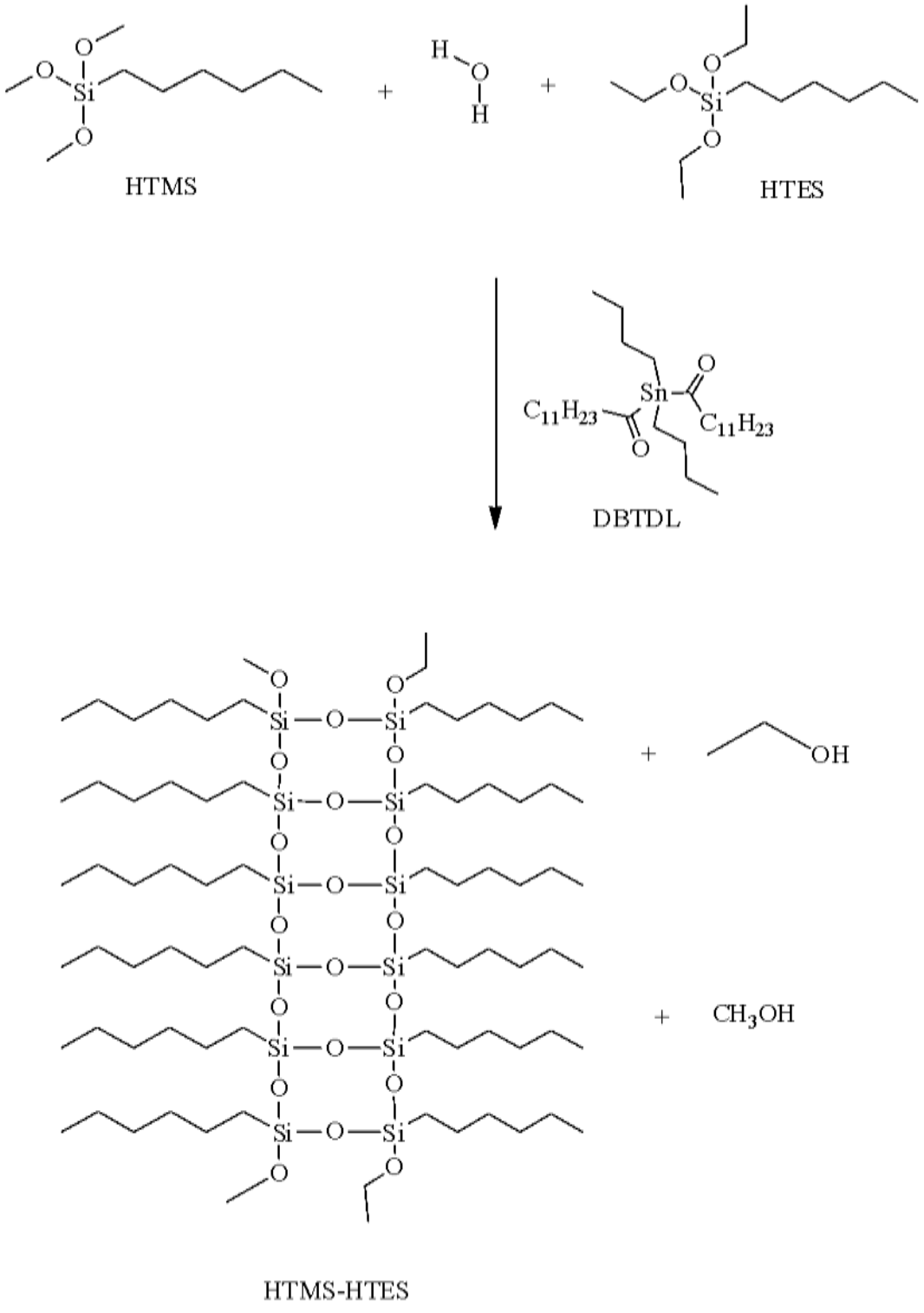

Figure 5. Schematic diagram of polycondensation of HTMS-HTES

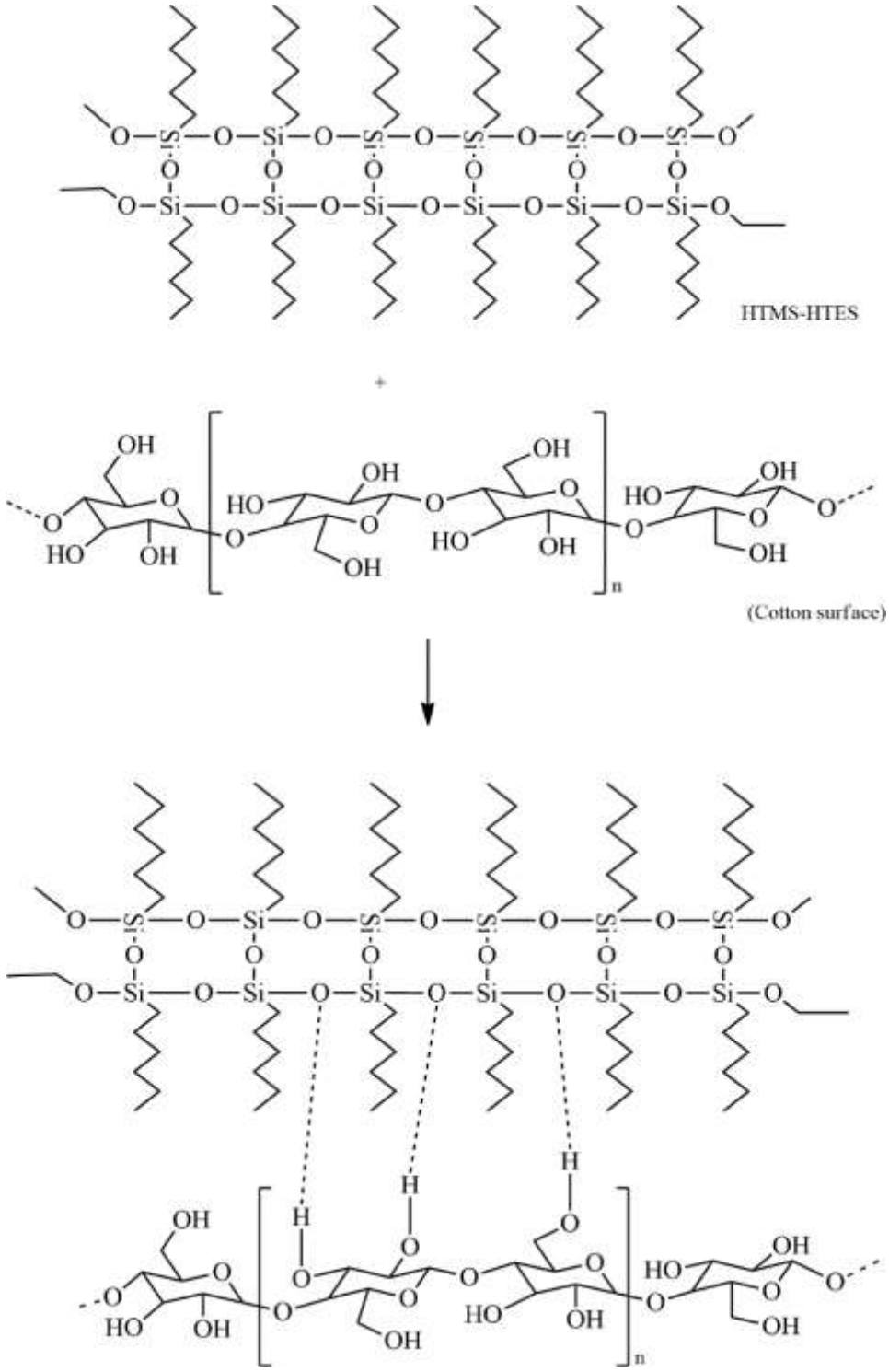

Figure 6. Schematic diagram of hydrogen bonding of HTMS-HTES coating solution with cotton fabric.

The coated fabrics with coating solution ratios of 1:0 exhibit little to no hydrophobicity when the water droplets did not produce WCA above 90° and penetrated the surface within a few minutes. On the other hand, all the other variations of the coating solution ratios applied to cotton and polyester fabrics demonstrated favourable hydrophobic properties even after an hour, as the water droplets stayed spherical and did not penetrate the fabric surface (Figure 8). In Figure 9, for cotton fabric, the highest WCA value of 135.41° was obtained at a ratio of 1:0.6 (HTMS: HTES). This indicates an improved hydro-phobicity of the coated fabric compared to the lower ratios tested. Likewise, for polyester fabric, the highest WCA value

of 132.28° was also achieved at a ratio of 1:0.6 (HTMS: HTES), indicating enhanced hydrophobicity compared to the lower ratios examined. The higher concentration of HTES in this ratio contributes to increased water repellences and a subsequent higher WCA value. The increase in the WCA can be attributed to the higher concentration of HTES, which introduces more hydrophobic hexyl functional groups in the coating [17]. These groups enhance the water repellences, resulting in a higher WCA value. However, at higher ratios such as 1:0.75 and 1:0.9, the WCA values decreased, which could be attributed to an excessive amount of HTES, leading to the formation of an uneven and less cohesive coating layer [21]. This unevenness may compromise the hydrophobicity, resulting in a lower WCA value. Additionally, the fixed curing time and temperature of 24 hours at room temperature for all the ratios may not be suitable for high HTES content applied to fabrics, which may require longer curing times and higher temperatures to optimize their properties [13].

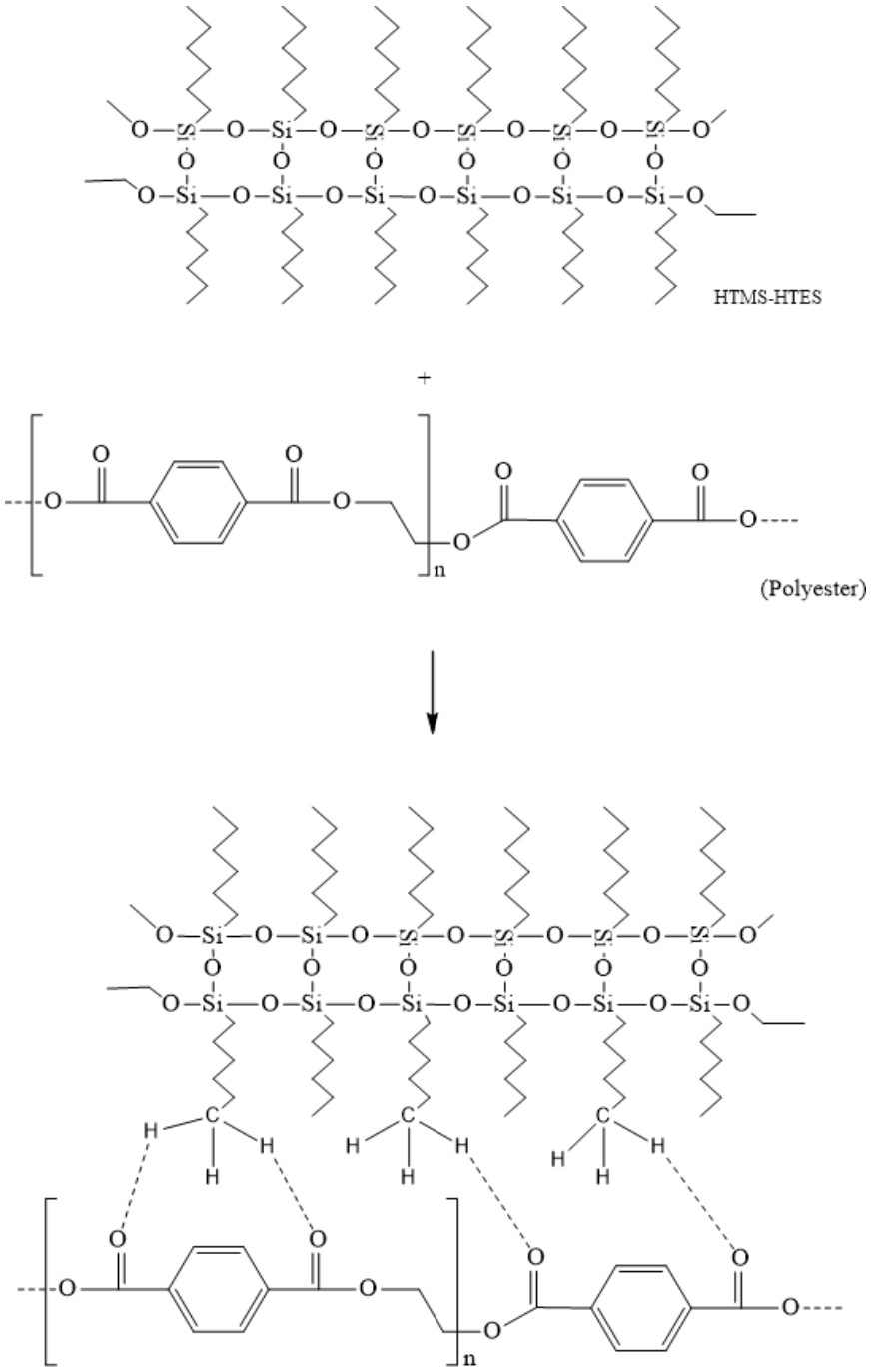

Figure 7. Schematic diagram of dipole-dipole bonding of HTMS-HTES coating solution with polyester fabric.

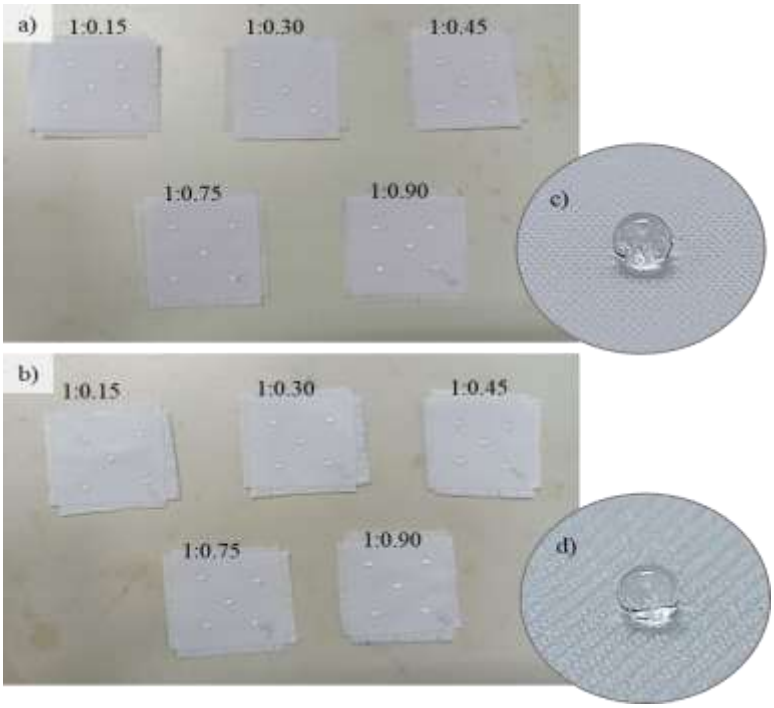

Figure 8. Water penetration test of HTMS-HTES coated a) cotton, and b) polyester using deionized water. Water droplets remain spherical and not penetrating c) cotton and d) polyester surface at 1:0.6 molar ratio.

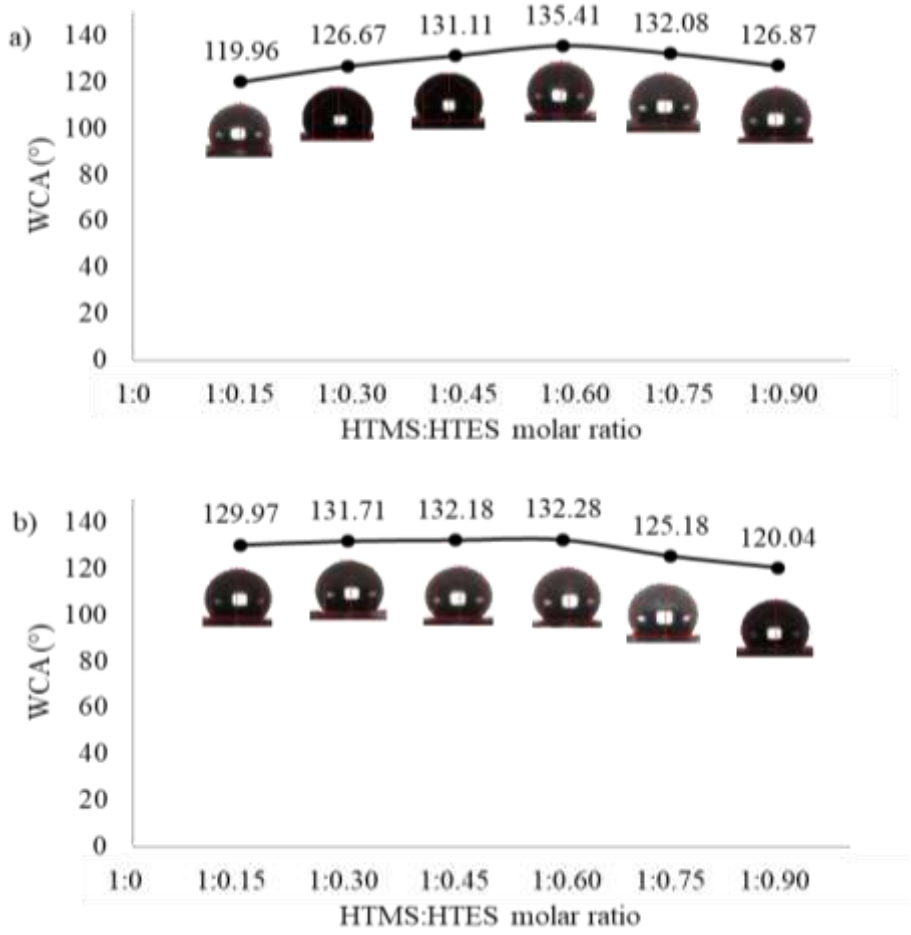

Figure 9. WCA versus HTMS to HTES molar ratio on coated a) cotton and b) polyester fabric surfaces.

FTIR Analysis

FTIR analysis was conducted on the raw HTMS, raw HTES, hydrolysed HTMS, and the hybrid HTMS-HTES coating solution. In the raw HTMS sample, peaks were detected at 2927.12 cm^{-1} and 1459.55 cm^{-1}, corresponding to CH stretching vibrations, indicating the presence of hydrocarbon groups [22]. The peak at 1191.45 cm^{-1} indicates Si-C stretching vibrations, suggesting the presence of silicon-carbon bonds. The peaks at 2840.19 cm^{-1} and 1081.66 cm^{-1} result from Si-OCH_3 asymmetric stretching of the silyl group, indicating the presence of silyl functional groups [13]. Additionally, the peak at 803.30 cm^{-1} suggests Si-O vibration modes, consistent with the presence of Si-OCH_3 groups in the raw HTMS sample [23].

In the raw HTES sample, similar to HTMS, a few low-intensity peaks are observed around 2973.18 cm^{-1} and 2926.30 cm^{-1}, corresponding to CH stretching vibrations. The series of peaks ranging from 1443.07 cm^{-1} to 1296 cm^{-1} suggest CH bending vibrations [22]. The peaks at 1189.20 cm^{-1}, 1166.31 cm^{-1}, and 1101.92 cm^{-1} represent Si-CH_2 stretching vibrations, indicating the presence of alkyl groups attached to the silicon atom. The peaks at 1075.91 cm^{-1} and 956.17 cm^{-1} suggest Si-OCH_2CH_3 groups [23]. Additionally, the peak at 783.32 cm^{-1} corresponds to Si-C stretching vibrations [24, 25], which indicates the presence of alkyl and silyl functional groups in the raw HTES sample.

The hydrolysed HTMS sample shows a broad peak at 3341.83 cm^{-1}, indicating O-H stretching vibrations resulting from the hydrolysis process. The peaks at 961.13 cm^{-1} and 1022.90 cm^{-1} represent the Si-OH bending and stretching vibrations, respectively, indicating the presence of Si-OH bonds [13]. Meanwhile, the peak at 903.90 cm^{-1} suggests Si-O stretching vibrations, while the peak at 792.87 cm^{-1} corresponds to Si-C stretching vibrations [23, 24].

In the hybrid HTMS-HTES coating solution, the broad peak at 3350.98 cm^{-1} indicates O-H stretching vibrations, which may be attributed to the presence of hydrolysed groups in the coating solution [26]. The peaks at 2926.60 cm^{-1} and 2859.63 cm^{-1} correspond to CH stretching vibrations, suggesting the presence of hydrocarbon groups [13]. The series of peaks ranging from 1458.64 cm^{-1} to 1391.25 cm^{-1} represent CH bending vibrations. The spectra for this sample show a few peaks indicating the presence of Si-$CH_2(CH_2)_4CH_3$, specifically at 1191.52 cm^{-1} and 1167.01 cm^{-1}. Peaks in this range do not change significantly among the spectra, as there is no reaction involving the alkyl group.

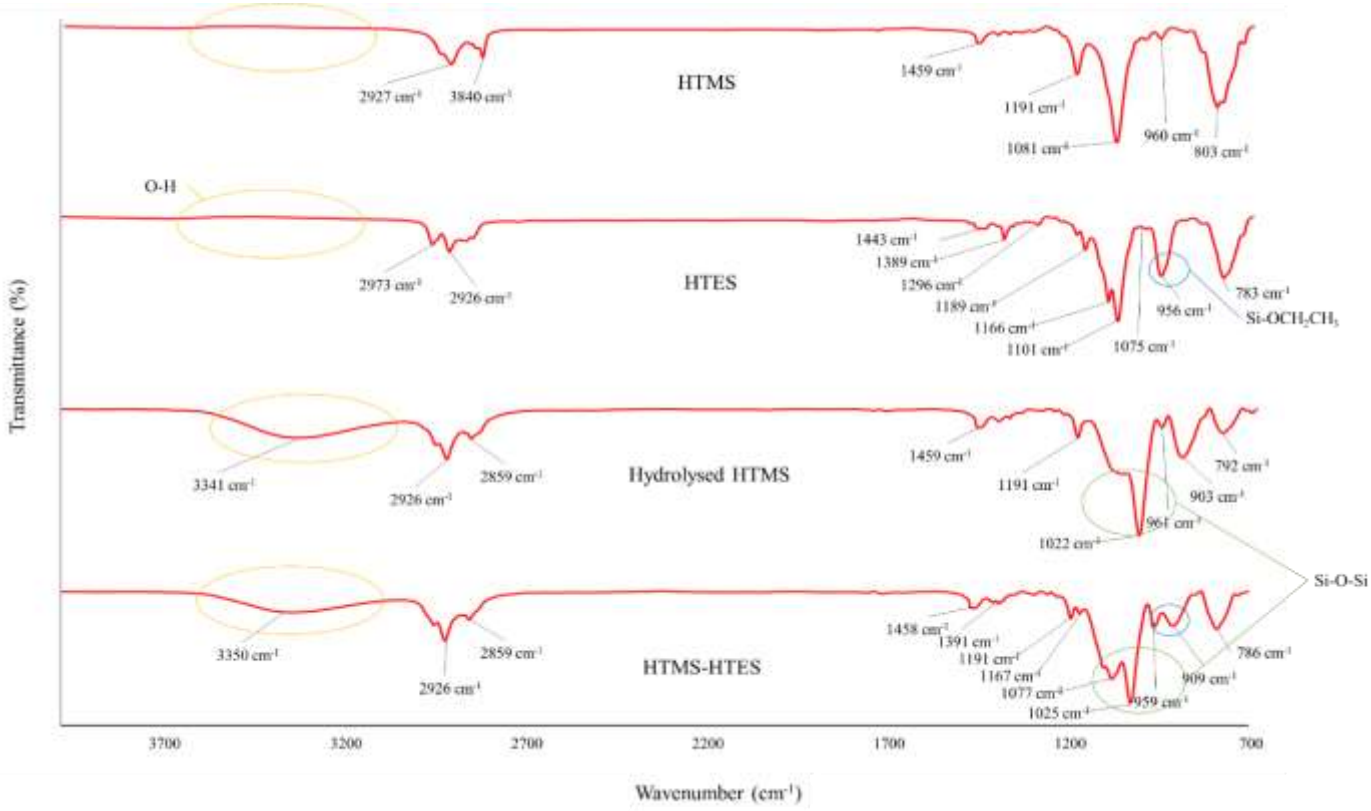

Figure 10. FTIR analysis of HTMS, HTES, hydrolysed HTMS and HTMS-HTES solution.

Meanwhile, the peaks at 1077.75 cm^{-1} and 1025.85 cm^{-1} correspond to Si–O–Si stretching vibrations, indicating the formation of siloxane bonds between HTMS and HTES [23]. The peaks at 1075.91, 1101.9 and 959.71 cm^{-1}, which are detected in the raw HTES spectra (highlighted black in Figure 10), decrease in intensity in the HTMS-HTES spectra, as these peaks indicate the Si-OCH_2CH_3 group, which detaches from Si to form ethanol (as illustrated in Figure 3) [23]. The peak at 959.71 cm^{-1} indicates Si-OH bending vibrations, the peak at 909.18 cm^{-1} suggests Si-O stretching vibrations, while the peak at 786.81 cm^{-1} corresponds to Si-C stretching vibrations [23, 24].

The differences in characteristic peaks (highlighted area in Figure 10) between the spectra demonstrate the occurrence of crosslinking reactions between HTMS and HTES. The formation of a crosslinked network is suggested by the large peak in the 3200–3500 cm^{-1} region in the hydrolysed HTMS and HTMS-HTES spectra, which corresponds to the stretching of O–H bonds [26, 27]. Moreover, the absence or reduction of characteristic peaks, from the raw HTMS and HTES in the FTIR spectra further supports the formation of new bonds due to crosslinked networks [26]. Table 2 highlights all the functional groups present in the raw HTMS, raw HTES, hydrolysed HTMS and HTMS-HTES hybrid coating solution.

Table 2. Wavenumber (cm^{-1}) of HTMS, HTES, hydrolysed HTMS, and HTMS-HTES solution.

Sample	Wavenumber (cm^{-1})	Functional Group
Raw HTMS	2927, 1459	CH stretching vibrations
	1191	Si-C stretching vibrations
	1081	Si-OCH_3 asymmetric stretching of silyl group
	803	Si-O vibration modes
Raw HTES	2973, 2926	CH stretching vibrations
	1443 – 1296	CH bending vibrations
	1189, 1166	Si-CH_2 stretching vibrations
	783	Si-C stretching vibrations
Hydrolysed HTMS	3341	O-H stretching vibrations
	2926	CH stretching vibrations
	1459	C-H absorption
	1022	Si-OH stretching vibrations
	961	Si-OH bending vibrations
	903	Si-O stretching vibrations
	792	Si-C stretching vibrations
Hybrid HTMS- HTES	3350	O-H stretching vibrations
	2926, 26859	CH stretching vibrations
	1458 – 1391	CH bending vibrations
	1191, 1167	Si-$CH_2(CH_2)_4CH_3$ group
	1077, 1025	Si-O-Si stretching vibrations
	959	Si-OH bending vibrations
	909	Si-O stretching vibrations
	786	Si-C stretching vibrations

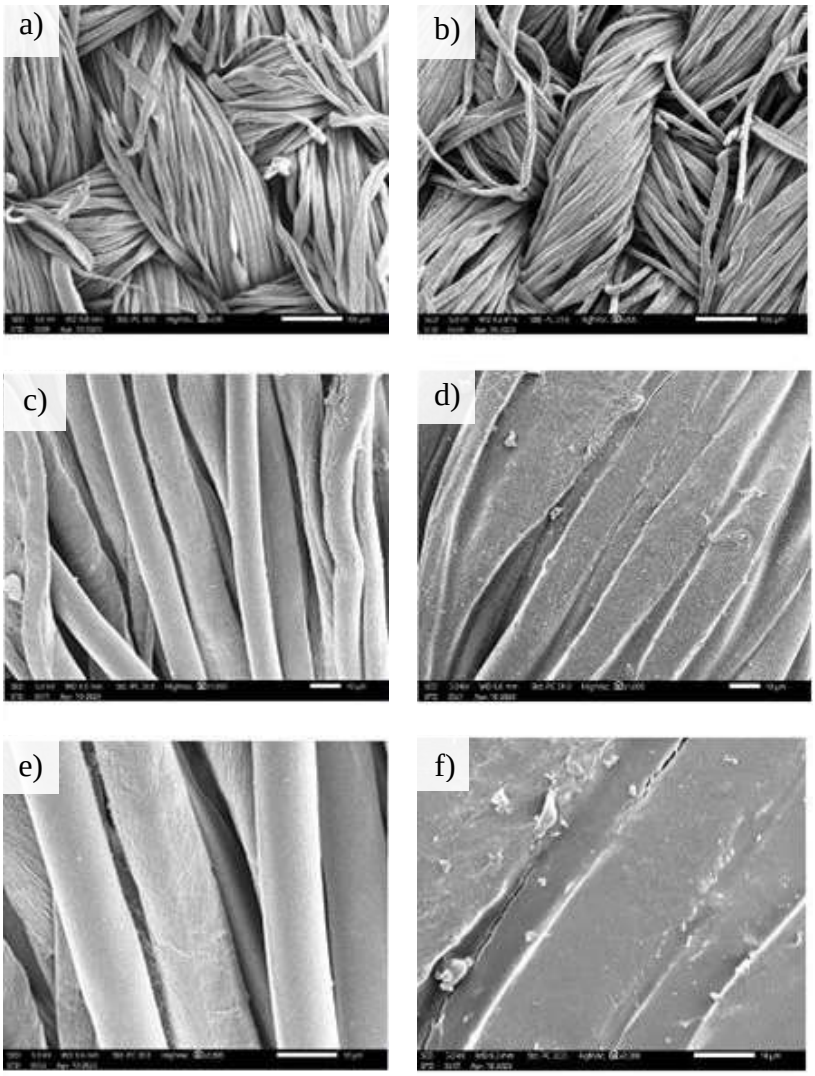

Figure 11. SEM images of cotton that is a) uncoated, b) coated at 200 µm magnification, c) uncoated, d) coated at 1000 µm magnification, and e) uncoated, f) coated at 2000 µm magnification.

SEM-EDX Analysis

The effect of coating on the morphology of both cotton and polyester fabrics was shown in Figure 11 and Figure 12, respectively. Figure 11 shows the surface of uncoated cotton fibre and HTMS-HTES coated cotton fabrics at magnifications of 200 µm, 1000 µm and 2000 µm. The untreated cotton fabric displays a distinct fibrous arrangement characterized by typical convolutions formed by the twisting of cellulose fibrils. [28, 29]. HTMS-HTES coatings show similar morphologies, with a thin layer added to the fibre surfaces, resulting in neighbouring fibres to bridge together and creating a relatively smooth surface, as portrayed in Figure 11 (b), (d), (f) for HTMS-HTES coating. This suggests successful coating of the fibres [30]. Since individual fibers remain visible in both coated cotton fabrics, it can be deduced that the coatings did not create a thick and consistent membrane on the fabric surface. [31].

Uncoated polyester fibres, Figure 12 (a), (c), and (e) observed under SEM, possess a smooth surface with a uniform texture and a cylindrical shape. Similar findings were also reported [26, 27]. The SEM images of HTMS-HTES coated polyester fabrics, Figure 12 (b), (d) and (f) also exhibit a uniform and smooth surface morphology at different magnifications. However, some areas of the coatings appear flaky. In addition, the differences in coating adhesion between the coated cotton and polyester fabrics can also be attributed to their respective surface properties. According to [29], cotton's surface texture is rougher and more porous in comparison to polyester, thus offering a larger surface area for coating adhesion. Conversely, the polyester surface properties which is smoother and a little hydrophobic may result in decreased adhesion of the coating. [32].

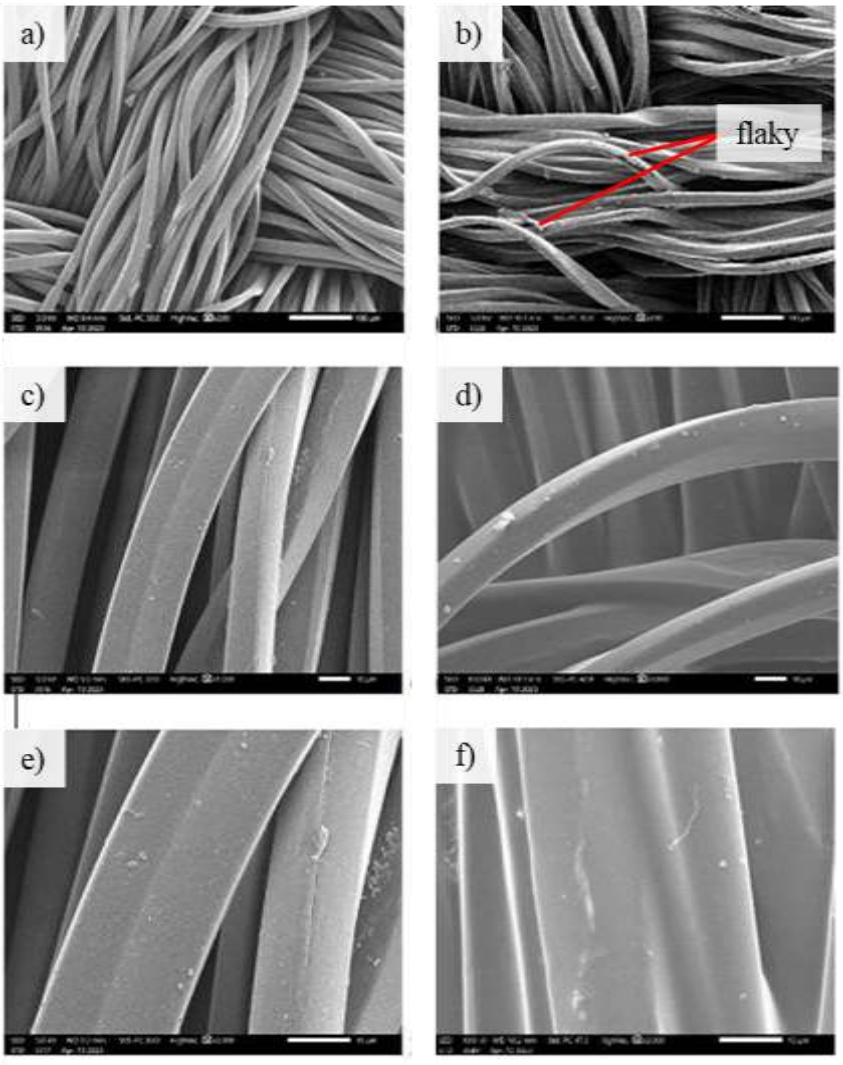

Figure 12. SEM images of polyester that is a) uncoated, b) HTMS-HTES coated at 200 µm magnification, c) uncoated, d) HTMS-HTES coated at 1000 µm magnification, and e) uncoated, f) HTMS-HTES coated at 2000 µm magnification.

Table 3. Carbon, oxygen and silicon mass and atom composition on fabric sample surfaces.

Element	Cotton			
	Uncoated		HTMS-HTES Coated	
	Mass %	Atom %	Mass %	Atom %
Carbon	47.60±0.43	54.75±0.50	54.88±0.39	62.85±0.45
Oxygen	52.40±0.94	45.25±0.81	40.69±0.68	34.98±0.58
Silica	-	-	4.43±0.21	2.17±0.10
Total	100.00	100.00	100.00	100.00
Element	**Polyester**			
	Uncoated		HTMS-HTES Coated	
	Mass %	Atom %	Mass %	Atom %
Carbon	59.92±0.51	66.57±0.56	59.65±0.46	6.77±0.35
Oxygen	40.08±0.95	33.43±0.79	33.58±0.71	28.73±0.61
Silica	-	-	6.77±0.35	3.30±0.17
Total	100.00	100.00	100.00	100.00

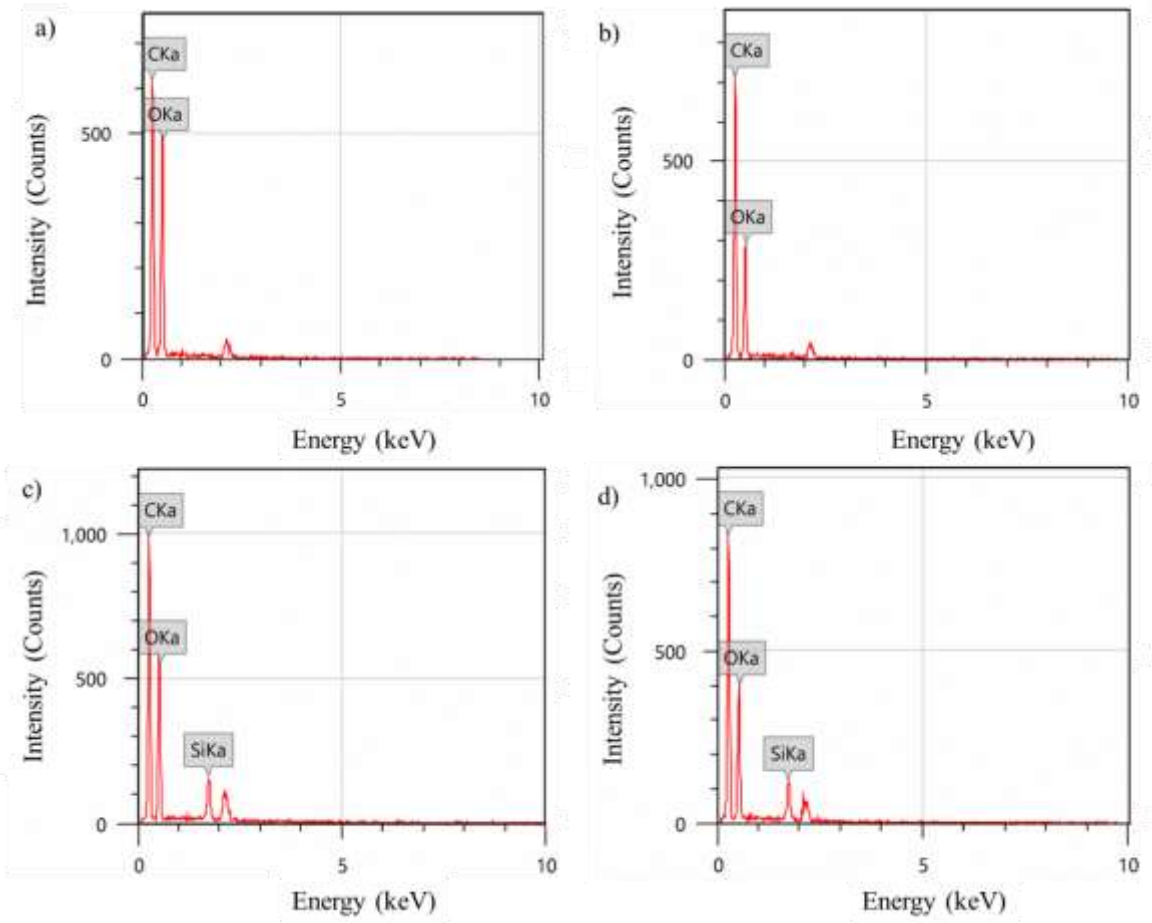

Figure 13. EDX analysis graph for a) uncoated cotton, b) uncoated polyester, c) coated cotton, and d) coated polyester.

EDX analysis shown in Figure 13 and Table 3, validates the presence of carbon, oxygen and silicon on the surfaces of HTMS: HTES coated fabrics, contrary to only carbon and oxygen in uncoated samples. These findings might be due to the silica chemically bonded to the fabric surface through a siloxane bond in the coating solution. Thus, indicates good adhesion of the coatings to the fabric surfaces and suggests a promising effective hydrophobicity [33].

CONCLUSION

A water-based hydrophobic coating for cotton and polyester fabrics was successfully synthesized by utilizing HTMS and HTES via a sol-gel method. Good hydrophobicity was achieved, with maximum WCA of 135.41° and 132.28° recorded for cotton and polyester fabric, respectively, at the optimum HTMS-HTES ratio of 1:0.6. HTMS underwent efficient hydrolysis using only water as a solvent in the presence of hydrochloric acid and was further integrated with HTES to form a hybrid coating solution. FTIR analysis confirmed the formation of Si–O–Si bond in the coating solution which is crucial to provide hydrophobicity and reduced band in the raw HTMS and HTES spectra indicating the effective reaction for hydrolysation. Additionally, SEM-EDX demonstrated good adhesion of the coatings to the fabric surfaces, with the addition of silica to the fabrics' surfaces contributing to the hydrophobic properties of the fabrics. These findings play a part in the development of more sustainable materials and methods with potential applications in self-cleaning surfaces, hydrophobic textiles, and various industries where hydrophobicity is a desirable trait.

ACKNOWLEDGEMENTS

The authors gratefully acknowledged the grant provided by Universiti Malaysia Pahang Al-Sultan Abdullah (UMPSA) under RDU Grant (Vote number: PGRS220385) that allowed this study to be carried out.

REFERENCES

1. Liao, X., Li, H., Zhang, L., Us, X., Lai, X. and Zeng, X. (2018) Superhydrophobic mGO/PDMS hybrid coating on polyester fabric for oil/water separation. *Progress in Organic Coatings*, **115**, 172–180.

2. Rafique, M. S., Tahir, M. B., Rafique, M. and Shakil, M. (2020) Photocatalytic nanomaterials for air purification and self-cleaning. *Nanotechnology and Photocatalysis for Environmental Applications*, 203–219.

3. Chen, X., Chen Y., Jin, T., He, L., Zeng, Y., Ma, Q. and Li, N. (2018) Fabrication of superhydrophobic coating from non-fluorine siloxanes via a one-pot sol–gel method. *Journal of Material Science Research*, **53(16)**, 11253–11264.

4. Dong, X., Gao, S., Huang, J., Li, S., Zhu, T., Cheng, Y., Zhao, Y., Chen, Z. and Lai, Y. (2019) A self-roughened and biodegradable superhydrophobic coating with UV shielding, solar-induced self-healing and versatile oil–water separation ability. *Journal of Materials Chemistry A*, **7(5)**, 2122–2128.

5. Xu, L., Wan, J., Yuan, X., Pan, H., Wang, L., Shen, Y. and Sheng, Y. (2022) Preparation of durable superamphiphobic cotton fabrics with self-cleaning and liquid repellency. *Journal of Adhesion Science and Technology*, **36(1)**, 1–20.

6. John, M. (2018) LCA Confirms Fluorine Textile Coating Risks. *Careers in Textiles*. November 30, 2018. [accessed 2022-08-11].

7. Liu, X., Wei, Y., Tao, F., Zhang, X., Gai, L. and Liu, L. (2022) All water-based superhydrophobic coating with reversible wettability for oil-water separation and wastewater purification. *Progress in Organic Coatings*, **165**, 106726.

8. Li, W., Qamar, S. A., Qamar, M., Basharat, A., Bilal, M. and Iqbal, H. M. N. (2021) Carrageenan-based nano-hybrid materials for the mitigation of hazardous environmental pollutants. *International Journal of Biological Macromolecules*, **190**, 700–712.

9. Nurul Hidayah, A. B., Hartina, M. Y., Wan Norfazilah, W. I. and Noreen Farzuhana, Z. (2023) Sol-gel finishing for protective fabrics. *Biointerface Research in Applied Chemistry*, **13(3)**, 283.

10. Matteo, P. and Plinio, I. (2021) Hydrophobic thin films from sol–gel processing: a critical review. *Materials*, **14(22)**, 6799.

11. Zhang, T., Fu, Y., Liang, M., Xu, L., He, C. and Lu, Z. (2022) Chemically and electrostatically double-crosslinked composite underwater adhesive. *Materials Letters*, **310**, 131132.

12. Zhong, S., Yi, L., Zhang, J., Xu, T., Xu, L., Zhang, X., Zuo, T. and Cai, Y. (2021) Self-cleaning and spectrally selective coating on cotton fabric for passive daytime radiative cooling. *Chemical Engineering Journal*, **407**, 127104.

13. Nur Nabilah, M. Z., Hartina, M. Y. and Wan Norfazilah, W. I. (2021) Synthesis of water-repellent coating for polyester fabric. *Emerging Science Journal*, **5(5)**, 747–754.

14. Nurul Hidayah, A. B., Wan Norfazilah, W. I., Hartina, M. Y. and Noreen Farzuhana, M. Z. (2024) Synthesis of a water-based TEOS–PDMS sol–gel coating for hydrophobic cotton and polyester fabrics. *New Journal of Chemistry*, **48**, 933–950.

15. ISO 3801:1977 (1977) Textiles – Woven Fabrics – Determination of Mass per Unit Length and Mass per Unit Area. *International Organization for Standardization, Geneva*, **401**, 1214.

16. Olivier, P., Marie-Christine, B., Elisa, Z. and Naceur, B. (2012) Hydrolysis-condensation kinetics of 3-(2-amino-ethylamino)propyl-trimethoxysilane. *Materials Science and Engineering: C.*, **32(3)**, 487–493.

17. Silvia, S., Tim, L., Giulia, R., Annamaria, V., Torsten, T. and Maira, R. P. (2023) Superhydrophobicity of polyester fabrics driven by functional sustainable fluorine-free silane-based coatings. *Gels*, **9(2)**, 109.

18. Kawamura, A., Takai, C., Fuji, M. and Shirai, T. (2016) Effect of solvent polarity and adsorbed water on reaction between hexyltriethoxysilane and fumed silica. *Colloids and Surfaces A: Physicochemical and Engineering Aspects*, **492**, 249–254.

19. Sergei, A. G. (2011) Structure and properties of textile materials. In *Handbook of Textile and Industrial Dyeing, eds. M. Clark, Elsevier: Amsterdam, Netherlands*.

20. Robert, J. Y. and Peter, A. L. (2011) Introduction to Polymers. *CRC Press, Florida*.

21. Marcin, P., Anna, S., Hieronim, M. and Katarzyna, M. (2020) Durable, highly hydrophobic modification of cotton fabric with fluorine-free polysiloxanes obtained via hydrosilylation and hydrothiolation reactions. *Cellulose*, **27(14)**, 8351–8367.

22. Xu, L., Wang, L., Shen, Y., Ding, Y. and Cai, Z. (2015) Preparation of hexadecyltrimethoxysilane-modified silica nanocomposite hydrosol and superhydrophobic cotton coating. *Fibers and Polymers*, **16(5)**, 1082–1091.

23. Philip, J. L. and Barry, A. (2013) Infrared analysis of organosilicon compounds. In book: *Silicon Compounds: Silanes & Silicones, 3rd ed., B. Arkles and G. L. Larson, Gelest Inc: Pennsylvania, United States.*

24. Lee, J., Kim, J., Kim, H., Bae, Y. M., Lee, K. H. and Cho, H. J. (2013) Effect of thermal treatment on the chemical resistance of polydimethylsiloxane for microfluidic devices. *Journal of Micromechanics and Microengineering*, **23(3)**, 035007.

25. Xia, X., Liu, J., Liu, Y., Lei, Z., Han, Y., Zheng, Z. and Yin, J. (2023) Preparation and characterization of biomimetic SiO_2-TiO_2-PDMS composite hydrophobic coating with self-cleaning properties for wall protection applications. *Coatings*, **13(2)**, 224.

26. Ahmed, A. I. and Adriaan, S. L. (2019) Kinetics of alkoxysilanes and organoalkoxysilanes polymerization: a review. *Polymers*, **11(3)**, 537.

27. Wan Aini, W. I., Wan Norfazilah, W. I., Aemi Syazwani, A. K. and Mohd Marsin, S. (2011) Preparation and characterization of a new sol–gel hybrid based tetraethoxysilane-polydimethylsiloxane as a stir bar extraction sorbent materials. *Journal of Sol-Gel Science and Technology*, **58(3)**, 602–611.

28. Billie, J. C. and Phyllis, G. T. (2001) Understanding Textiles. *Prentice Hall, New Jersey*.

29. Justyna, S., Waldemar, M., Stanislawa, K., Anita, J., Tomasz, R., Aleksandra, S. and Beata, G. (2020) Beeswax-modified textiles: method of preparation and assessment of antimicrobial properties. *Polymers*, **12(2)**, 344.

30. Arsheen, M., Rajiv, P. and Xin, W. (2017) Coating of TPU-PDMS-TMS on polycotton fabrics for versatile protection. *Polymers*, **9(12)**, 660.

31. Franco, F. and Monica, P. (2015) Modification of surface energy and wetting of textile fibers. In *Wetting and Wettability*; *eds. M. Aliofkhazraei, InTech: London, United Kingdom*.

32. Raha, S., Nikolay, B., Amine, M. L., Suraj, S., Igor, L. and Sergiy, M. (2020) Adhesion and stability of nanocellulose coatings on flat polymer films and textiles. *Molecules*, **25(14)**, 3238.

33. George, S. (2004) Infrared and Raman Characteristic Group Frequencies: Tables and Charts. *John Wiley & Sons, New Jersey*.